

Phase-field elasticity model based on mechanical jump conditions

Daniel Schneider¹ · Oleg Tschukin² · Abhik Choudhury³ ·
Michael Selzer^{1,2} · Thomas Böhlke⁴ · Britta Nestler^{1,2}

Received: 24 October 2014 / Accepted: 9 March 2015 / Published online: 31 March 2015
© Springer-Verlag Berlin Heidelberg 2015

Abstract Computational models based on the phase-field method typically operate on a mesoscopic length scale and resolve structural changes of the material and furthermore provide valuable information about microstructure and mechanical property relations. An accurate calculation of the stresses and mechanical energy at the transition region is therefore indispensable. We derive a quantitative phase-field elasticity model based on force balance and Hadamard jump conditions at the interface. Comparing the simulated stress profiles calculated with Voigt/Taylor (Annalen der Physik 274(12):573, 1889), Reuss/Sachs (Z Angew Math

Mech 9:49, 1929) and the proposed model with the theoretically predicted stress fields in a plate with a round inclusion under hydrostatic tension, we show the quantitative characteristics of the model. In order to validate the elastic contribution to the driving force for phase transition, we demonstrate the absence of excess energy, calculated by Durga et al. (Model Simul Mater Sci Eng 21(5):055018, 2013), in a one-dimensional equilibrium condition of serial and parallel material chains. To validate the driving force for systems with curved transition regions, we relate simulations to the Gibbs-Thompson equilibrium condition (Johnson and Alexander, J Appl Phys 59(8):2735, 1986).

✉ Daniel Schneider
daniel.schneider@kit.edu

Oleg Tschukin
oleg.tschukin@hs-karlsruhe.de

Abhik Choudhury
abhiknc@materials.iisc.ernet.in

Michael Selzer
michael.selzer@kit.edu

Thomas Böhlke
thomas.boehlke@kit.edu

Britta Nestler
britta.nestler@kit.edu

¹ Institute of Applied Materials (IAM-CMS), Karlsruhe Institute of Technology (KIT), Kaiserstrasse 12, 76131 Karlsruhe, Germany

² Institute of Materials and Processes, Karlsruhe University of Applied Science, Moltkestrasse 30, 76133 Karlsruhe, Germany

³ Department of Materials Engineering, Indian Institute of Science, Bangalore 560 012, India

⁴ Chair for Continuum Mechanics, Institute of Engineering Mechanics, Karlsruhe Institute of Technology (KIT), Kaiserstrasse 12, 76131 Karlsruhe, Germany

Keywords Phase-field · Elasticity · Jump-conditions · Microstructure evolution · Heterogeneous systems · Interfacial excess energy

1 Introduction

The modeling of microstructure evolution has become very essential in material science and physics. Phase-field methods become increasingly important with its capability to simulate complicated morphological evolution, in response to the evolution of the different thermodynamic physical fields, while incorporating the influence of capillarity. Therefore the phase-field method has been established for simulating the microstructural evolution in a wide variety of material processes, such as solidification, solid-state phase transformations, precipitate growth and coarsening, martensitic transformations and grain growth [5]. In the phase-field method, we typically map a given sharp interface free boundary problem onto a diffuse interface that is constructed out of smoothly varying phase-field order parameters. The dif-

ferent physical fields (concentration, stress, strain etc.) vary continuously across the constructed interface following the variation of the order parameters. Such a construction is advantageous because it obviates the requirement to track the interface between the phase boundaries during microstructural evolution [6], as morphological evolution is implicitly described through the spatiotemporal evolution of the different order parameters. Concomitant with the evolution of the phase-fields the different physical fields related to the mass, momentum and energy are self-consistently described using appropriate conservation equations. Although the process is elegant, appropriate care must be exercised in the construction of the evolution equations of the phase-fields and the conservation equations, which generally require homogenization of the variables exhibiting jumps across the interface in the original sharp interface problem. In the absence of the correct homogenization scheme, artificial jumps in the continuous variables could be introduced in the problem, which then leads to an incorrect mapping with respect to the actual free-boundary problem.

Describing solid state transformation processes or predicting microstructure and mechanical property relations, an accurate calculation of the stresses and mechanical energy at the transition region is indispensable. This requires that the effective material parameters are defined in the diffuse-interface regions in non-homogeneous materials, which is usually performed by homogenization of the material parameters using smooth varying functions constructed out of the spatially varying phase-fields. In the phase-field community, there are several known homogenization approaches, see [7] for an overview of approaches. Khachaturyan's model [8] is widely established in phase-field applications. In absence of nonelastic strains, the model of Khachaturyan is equal to the Voigt/Taylor (VT) homogenization scheme [1] between locally overlapping phases. The main assumption of the VT approach is that the strains of overlapping phases are the same. With an order parameter ϕ the stress in the isostrain two phase case reads as

$$\sigma^{VT}(\phi) = \mathcal{C}^\alpha [\epsilon - \tilde{\epsilon}^\alpha] h(\phi) + \mathcal{C}^\beta [\epsilon - \tilde{\epsilon}^\beta] (1 - h(\phi)). \quad (1)$$

ϵ is the local strain, which in turn depends on the gradient of displacement field $(\nabla \mathbf{u})_{ij} = \partial u_i / \partial x_j$ by $\epsilon = (\nabla \mathbf{u} + (\nabla \mathbf{u})^T) / 2$, and $\sigma_{ij} = (\mathcal{C}[\epsilon - \tilde{\epsilon}])_{ij} = C_{ijkl}(\epsilon_{kl} - \tilde{\epsilon}_{kl})$ is the particular stress component using the Einstein summation convention. $\tilde{\epsilon}^\alpha$ and \mathcal{C}^α represent the local nonelastic strain and the stiffness tensor of phase α . $h(\phi)$ is the interpolation function which is in the simplest case $h(\phi) = \phi$. This approach is employed in [9–12]. Assuming equal stresses in the transition region results in stress, due to the Reuss/Sachs (RS) [2] approximation

$$\sigma^{RS}(\phi) = [\mathcal{S}^\alpha h(\phi) + \mathcal{S}^\beta (1 - h(\phi))]^{-1} \times \left[\epsilon - \left(\tilde{\epsilon}^\alpha h(\phi) + \tilde{\epsilon}^\beta (1 - h(\phi)) \right) \right], \quad (2)$$

where \mathcal{S}^α is the compliance tensor of phase α . This local homogenization scheme has been discussed by Steinbach [13] and Apel et al. [14]. Ammar et al. [7] propose a Hashin-Shtrikman homogenization between locally existing phases and present an accurate comparison between Khachaturyan's, VT, RS and their own approach. In a recent publication, Durga et al. [3] investigate the excesses of the stress, strain and the elastic energy for both, the VT and RS interpolation to estimate the material properties at the interface. As a result of the calculations, it is clear that under conditions of uniaxial loading of the interface, the RS interpolation delivers an excess free interface, while the conditions of a parallel material circuit with a complete shear loading require a VT interpolation such that there is no excess contribution from the bulk energy density to the surface energy. With this motivation, the respective paper proposes a model by combining the VT and RS interpolation schemes wherein, a VT interpolation is imposed, in order to derive the tangential stress component and the RS scheme is utilized to determine the stress components on the normal plane. Although, the model promises a new perspective, there is a problem with the associated formulation. In the description of the model, the stress, strain and stiffness tensor need to be transformed into a coordinate system consisting of the interfacial normal and of another orthogonal direction in the plane of separation of the phases. To derive a solution, the transformed state of stress is assumed to be a principal state. This is a physically unrealistic situation, given there exist purely shear problems in materials science involving precipitate growth. Hence, the assumption is restrictive and makes the model not globally applicable.

VT and RS methods offer approximations for two limits of the real material parameters for locally overlapping phases. When using these schemes, the approximation of elastic constants is only valid in one-dimensional special cases. The VT limit provides an exact stiffness for a one-dimensional parallel material circuit of different materials and the RS approximation does this for a one-dimensional material chain. For all other cases, jump conditions at the transition zones, from one material to the other, have to be fulfilled in order to calculate the correct stresses or strains.

The equilibrium jump condition is a force balance in the normal direction of the interface and the Hadamard condition in the tangential direction [15]. Based on these jump conditions, we formulate a quantitative phase-field elasticity model. Comparing the simulated stress and strain profiles with the theoretically predicted fields in a one dimensional serial and parallel material chain setup as well as for a plate with a round inclusion under hydrostatic tension, we

highlight the quantitative characteristics of the model. Kim et al. [16], Plapp [17] Choudhury and Nestler [18] pointed out for solidification processes, that a driving force, which contains only homogeneous variables, avoid the interfacial excess energy. The proposed model uses normal components of the stresses and tangential components of the strains, for the definition of consistent potential type and consequently for the formulation of the driving force. In order to validate the elastic contribution of the driving force, we generate one dimensional equilibrium conditions in the normal and tangential directions and demonstrate the absence of excess energy.

2 Model formulation

2.1 Phase-field

The model is based on a generalized phase-field approach for microstructure evolution in multi-phase and multi-component systems [19]. In a two phase system, only one order parameter ϕ is needed, which represents the volume fraction of phase α . Accordingly the volume fraction of phase β is $1 - \phi$. The energy functional can be expressed in the form

$$\mathcal{F}(\phi, \nabla\phi, \epsilon) = \int_V \left(\epsilon a(\nabla\phi) + \frac{1}{\epsilon} \omega_{ob}(\phi) + f_{el}(\phi, \epsilon) \right) dV, \tag{3}$$

where $f_{el}(\phi, \epsilon)$ denotes an elastic energy density contribution as a function of the local strain ϵ . The gradient energy density in Eq. (3) reads $a(\nabla\phi) = \gamma_{\alpha\beta} |\nabla\phi|^2$, as presented in [19], where $\gamma_{\alpha\beta}$ represents the surface energy density between the phases α and β . We further use an obstacle-type formulation $\omega_{ob} = 16\gamma_{\alpha\beta}\phi(1 - \phi)/\pi^2$ as the potential. ϵ is a small length scale parameter related to the diffuse interface thickness. Following the Ginzburg–Landau analysis, the interface traction $\dot{\phi} = \partial\phi/\partial t$ is proportional to a variational derivative of the functional (3) with respect to the order parameter ϕ . The proportionality constant is the mobility of the interface $1/\tau$. The evolution equation for the order parameter ϕ is obtained according to

$$\tau \epsilon \dot{\phi} = - \frac{\delta \mathcal{F}}{\delta \phi}, \tag{4}$$

where the variational derivative writes as

$$\frac{\delta}{\delta \phi} = \frac{\partial}{\partial \phi} - \nabla \cdot \frac{\partial}{\partial \nabla \phi}. \tag{5}$$

We solve explicitly the momentum balance equation,

$$\rho \ddot{\mathbf{u}} = \nabla \cdot \boldsymbol{\sigma}, \tag{6}$$

for the evolution of displacement field \mathbf{u} , until the mechanical equilibrium $\rho \ddot{\mathbf{u}} = \mathbf{0}$ is reached. ρ is the mass density and $(\nabla \cdot \boldsymbol{\sigma})_i = \partial \sigma_{ij} / \partial x_j$ defines the stress divergence. $\ddot{\mathbf{u}} = \partial^2 \mathbf{u} / \partial t^2$ is the second partial time derivative of \mathbf{u} .

2.2 Solid–solid jump conditions

The mechanical jump conditions for a bounded solid–solid transition are the underlying physical equations of the proposed model. For a sharp interface theory in the case of singular surface, the force balance reads [15]

$$(\boldsymbol{\sigma}^\alpha - \boldsymbol{\sigma}^\beta) \mathbf{n} = \llbracket \boldsymbol{\sigma} \rrbracket \mathbf{n} = \mathbf{0}, \tag{7}$$

with the normal vector \mathbf{n} at the interface between α and β phase and the corresponding jump of stresses $\llbracket \boldsymbol{\sigma} \rrbracket$. The traction vector $\mathbf{t}_{lr} = \boldsymbol{\sigma}^\alpha \mathbf{n} = \sigma_{ij}^\alpha n_j$ on the left and $\mathbf{t}_{rr} = \boldsymbol{\sigma}^\beta \mathbf{n}$ on the right of the transition zone are continuous functions at the singular surface. Apart from the continuity of the displacement field \mathbf{u} , the Hadamard jump condition follows for $\nabla \mathbf{u}$ accordingly to [15]

$$\llbracket \nabla \mathbf{u} \rrbracket = \mathbf{a} \mathbf{n}^T. \tag{8}$$

$(\mathbf{a} \mathbf{n}^T)_{ij} = a_i n_j$ is the dyadic product of an arbitrary vector \mathbf{a} and the normal vector \mathbf{n} . The jump of the deformation gradient $\llbracket \nabla \mathbf{u} \rrbracket$ vanishes in the tangential direction and implies a no slip boundary condition. If we multiply two tangential vectors \mathbf{t} and \mathbf{s} with $\langle \mathbf{t}, \mathbf{n} \rangle = t_i n_i = 0$ and $\langle \mathbf{s}, \mathbf{n} \rangle = 0$ it can be seen, that $\llbracket \nabla \mathbf{u} \rrbracket \mathbf{t} = \mathbf{0}$ and $\llbracket \nabla \mathbf{u} \rrbracket \mathbf{s} = \mathbf{0}$.

2.3 Energy formulation

As seen in the previous section the jump conditions (7) and (8) depend on the interface orientation \mathbf{n} . The basic idea of our approach is to transform the stresses and strains to the basis fixed on \mathbf{n} and then to calculate the energy using only homogeneous variables, which are given by the jump conditions (7) and (8). For the manageability of the calculations, we neglect the eigenstrains $\tilde{\epsilon}$ in the first step and include them afterwards.

The base \mathbf{B} , which is fixed due to \mathbf{n} , is given by $\mathbf{B} = \{\mathbf{n}, \mathbf{t}, \mathbf{s}\}$, with $\langle \mathbf{n}, \mathbf{t} \rangle = 0$, $\langle \mathbf{n}, \mathbf{s} \rangle = 0$, $\langle \mathbf{t}, \mathbf{s} \rangle = 0$ and the normal vector of the transition region

$$\mathbf{n} = \frac{\nabla \phi}{|\nabla \phi|}, \tag{9}$$

with $|\nabla \phi| = \sqrt{\langle \nabla \phi, \nabla \phi \rangle}$ as the norm of $\nabla \phi$. The transformation of the stress tensor $\boldsymbol{\sigma}$ to the base coordinate system \mathbf{B} writes as

$$\sigma_B = \mathbf{Q}\sigma\mathbf{Q}^T = \begin{pmatrix} \sigma_{nn} & \sigma_{nt} & \sigma_{ns} \\ \sigma_{nt} & \sigma_{tt} & \sigma_{ts} \\ \sigma_{ns} & \sigma_{ts} & \sigma_{ss} \end{pmatrix}, \tag{10}$$

\mathbf{Q} is a locally defined orthonormal matrix

$$\mathbf{Q} = \begin{pmatrix} n_1 & n_2 & n_3 \\ t_1 & t_2 & t_3 \\ s_1 & s_2 & s_3 \end{pmatrix}. \tag{11}$$

The traction vector $\mathbf{t}_{tr} = \sigma_B \mathbf{n}$ can now be written in the transformed coordinate system

$$\mathbf{t}_{tr} = \begin{pmatrix} t_n \\ t_t \\ t_s \end{pmatrix} = \begin{pmatrix} \sigma_{nn} & \sigma_{nt} & \sigma_{ns} \\ \sigma_{nt} & \sigma_{tt} & \sigma_{ts} \\ \sigma_{ns} & \sigma_{ts} & \sigma_{ss} \end{pmatrix} \begin{pmatrix} 1 \\ 0 \\ 0 \end{pmatrix} = \begin{pmatrix} \sigma_{nn} \\ \sigma_{nt} \\ \sigma_{ns} \end{pmatrix}. \tag{12}$$

With the previous relations formed in the coordinate system \mathbf{B} , the continuity of the traction vector \mathbf{t}_{tr} in the normal direction results in the continuity of stress components σ_{nn} , σ_{nt} and σ_{ns} . Similarly the Hadamard condition (8) leads to the continuity of the strain components ϵ_{tt} , ϵ_{ss} and ϵ_{ts} . Thereby the jump conditions (7) and (8) are equivalent to

$$\begin{aligned} \llbracket \sigma_B \rrbracket &= \begin{pmatrix} 0 & 0 & 0 \\ 0 & \llbracket \sigma_{tt} \rrbracket & \llbracket \sigma_{ts} \rrbracket \\ 0 & \llbracket \sigma_{ts} \rrbracket & \llbracket \sigma_{ss} \rrbracket \end{pmatrix}, \\ \llbracket \epsilon_B \rrbracket &= \begin{pmatrix} \llbracket \epsilon_{nn} \rrbracket & \llbracket \epsilon_{nt} \rrbracket & \llbracket \epsilon_{ns} \rrbracket \\ \llbracket \epsilon_{nt} \rrbracket & 0 & 0 \\ \llbracket \epsilon_{ns} \rrbracket & 0 & 0 \end{pmatrix}. \end{aligned} \tag{13}$$

This means, that in a jump between the phases, the normal components of σ_B and the tangential components of ϵ_B are homogeneous. Using the Voigt notation, the transformation of stresses and strains reads

$$\sigma_B^v = \mathbf{M}_\sigma^v \sigma^v, \tag{14}$$

$$\epsilon_B^v = \mathbf{M}_\epsilon^v \epsilon^v \tag{15}$$

with \mathbf{M}_σ^v and \mathbf{M}_ϵ^v as transformation matrices (see Appendix for the definition) and the corresponding variables in Voigt notation

$$\sigma^v = (\sigma_{xx}, \sigma_{yy}, \sigma_{zz}, \sigma_{yz}, \sigma_{xz}, \sigma_{xy})^T, \tag{16}$$

$$\epsilon^v = (\epsilon_{xx}, \epsilon_{yy}, \epsilon_{zz}, 2\epsilon_{yz}, 2\epsilon_{xz}, 2\epsilon_{xy})^T. \tag{17}$$

We reorder the components of the strain and stress vectors to separate the normal and tangential components and define

$$\epsilon_B^\alpha := (\underbrace{\epsilon_{nn}^\alpha, 2\epsilon_{ns}^\alpha, 2\epsilon_{nt}^\alpha}_{\epsilon_n^\alpha}, \underbrace{\epsilon_{tt}^\alpha, \epsilon_{ss}^\alpha, 2\epsilon_{ts}^\alpha}_{\epsilon_t^\alpha})^T = (\epsilon_n^\alpha, \epsilon_t^\alpha)^T, \tag{18}$$

$$\sigma_B^\alpha := (\underbrace{\sigma_{nn}^\alpha, \sigma_{ns}^\alpha, \sigma_{nt}^\alpha}_{\sigma_n^\alpha}, \underbrace{\sigma_{tt}^\alpha, \sigma_{ss}^\alpha, \sigma_{ts}^\alpha}_{\sigma_t^\alpha})^T = (\sigma_n^\alpha, \sigma_t^\alpha)^T. \tag{19}$$

The superscript α denotes that the particular variable is non homogeneous and dependent on the particular phase. The homogeneous variables are denoted without a superscript and are defined according to the jump conditions (13). Because of this reformulation, we permute the rows of the transformation matrices and derive the following expressions from Eqs. (14) and (15)

$$\sigma_B^\alpha = \mathbf{M}_\sigma \sigma^v, \tag{20}$$

$$\epsilon_B^\alpha = \mathbf{M}_\epsilon \epsilon^v. \tag{21}$$

Thereby, are \mathbf{M}_σ and \mathbf{M}_ϵ transformation matrices (see Appendix for the definition) for stresses and strains directly in the used base notation, which is defined by Eqs. (18) and (19). Using that notation and the relation $\mathbf{M}_\sigma^{-1} = \mathbf{M}_\epsilon^T$ [20], the free elastic energy for the bulk phase α can be written in the form

$$\begin{aligned} f_{el}^\alpha(\epsilon^v) &= \frac{1}{2} \langle \epsilon^v, \mathbf{C}^\alpha \epsilon^v \rangle = \frac{1}{2} \langle \mathbf{M}_\epsilon^{-1} \epsilon_B^\alpha, \mathbf{C}^\alpha \mathbf{M}_\epsilon^{-1} \epsilon_B^\alpha \rangle \\ &= \frac{1}{2} \langle \epsilon_B^\alpha, \underbrace{\mathbf{M}_\sigma \mathbf{C}^\alpha \mathbf{M}_\sigma^T}_{=: \mathbf{C}_B^\alpha} \epsilon_B^\alpha \rangle = f_{el}^\alpha(\epsilon_B^\alpha), \end{aligned} \tag{22}$$

with \mathbf{C}^α as the stiffness tensor of phase α in the Voigt notation. In order to simplify the derivations, we break the stiffness tensor into different blocks

$$\mathbf{C}_B^\alpha = \begin{pmatrix} C_{nn}^\alpha & C_{nt}^\alpha \\ C_{tn}^\alpha & C_{tt}^\alpha \end{pmatrix}, \tag{23}$$

where C_{nn}^α and C_{tt}^α are symmetric matrices of 3×3 dimensions and C_{tn}^α is a 3×3 matrix with $C_{tn}^\alpha = C_{nt}^{\alpha T}$. With the previous notations in Eqs. (18), (19) and (23), we rewrite the expression of the free elastic energy of the α phase as a sum of scalar products in the appropriate spaces

$$\begin{aligned} f_{el}^\alpha(\epsilon_B^\alpha) &= \frac{1}{2} \langle \epsilon_B^\alpha, \mathbf{C}_B^\alpha \epsilon_B^\alpha \rangle \\ &= \frac{1}{2} (\langle \epsilon_n^\alpha, C_{nn}^\alpha \epsilon_n^\alpha \rangle + \langle \epsilon_n^\alpha, C_{nt}^\alpha \epsilon_t \rangle \\ &\quad + \langle \epsilon_t, C_{tn}^\alpha \epsilon_n^\alpha \rangle + \langle \epsilon_t, C_{tt}^\alpha \epsilon_t \rangle). \end{aligned} \tag{24}$$

The elastic energy $f_{el}^\alpha(\epsilon_B^\alpha)$ is a function of homogeneous ϵ_t and non homogeneous variables ϵ_n^α . The discontinuity of ϵ_n^α is indicated by the superscript α . Now we are able to dissolve the whole dependence of ϵ_n^α . This can be done in two ways. We can replace ϵ_n in Eq. (24) for the elastic potential energy, but then we have to deal with excess energy correction terms [16] in order to receive a quantitative formulation. Another way is to follow the approach of Plapp [17], Choudhury and Nestler [18] to generate a potential which is only dependent on homogeneous system variables. Therefore we

consider the elastic contribution of the driving force for phase transition.

2.4 Elasticity driving force contribution

The traction of the particular order parameter is proportional to the variational derivative of the functional $\mathcal{F}(\phi, \nabla\phi, \epsilon)$, which is given by Eq. (3). The derivatives of the gradient energy density $a(\nabla\phi)$ and the potential $\omega(\phi)$ are described e.g. in [19] or [18]. Here we are focusing only on the derivative $\partial/\partial\phi$ for the variation of the elastic contribution of $\mathcal{F}(\phi, \nabla\phi, \epsilon)$.

The interface gives the orientation of the reference coordinate system by the gradient vector $\nabla\phi$ which in turn represents the directions in which stresses and strains are decomposed, using Eqs. (18) and (19). The driving force is the total elastic energy of the system, which writes as the interpolated sum of the elastic energies of two phases weighted with the smooth function $h(\phi)$ and $h(1 - \phi) = 1 - h(\phi)$, respectively. According to Eq. (24), the energy of the phases can be expressed as

$$\begin{aligned}
 f_{el}^\alpha &= \frac{1}{2} \left(\langle \epsilon_n^\alpha, C_{nn}^\alpha \epsilon_n^\alpha \rangle + \langle \epsilon_n^\alpha, C_{nt}^\alpha \epsilon_t \rangle + \langle \epsilon_t, C_{tn}^\alpha \epsilon_n^\alpha \rangle \right. \\
 &\quad \left. + \langle \epsilon_t, C_{tt}^\alpha \epsilon_t \rangle \right), \\
 f_{el}^\beta &= \frac{1}{2} \left(\langle \epsilon_n^\beta, C_{nn}^\beta \epsilon_n^\beta \rangle + \langle \epsilon_n^\beta, C_{nt}^\beta \epsilon_t \rangle + \langle \epsilon_t, C_{tn}^\beta \epsilon_n^\beta \rangle \right. \\
 &\quad \left. + \langle \epsilon_t, C_{tt}^\beta \epsilon_t \rangle \right), \\
 f_{el} &= f_{el}^\alpha h(\phi) + f_{el}^\beta h(1 - \phi). \tag{25}
 \end{aligned}$$

We note that the superscripts α, β are mentioned only on the non-homogeneous variables. The elastic driving force contribution is given by the variation of f_{el} with respect to ϕ

$$\frac{\delta f_{el}}{\delta \phi} = \frac{\partial f_{el}}{\partial \phi} - \nabla \cdot \frac{\partial f_{el}}{\partial \nabla \phi}. \tag{26}$$

To perform the first part of the variation, we just note the following interpolations that must result out of the jump condition in normal direction (see Eqs. (7) and (12)) namely

$$\epsilon_n = \epsilon_n^\alpha h(\phi) + \epsilon_n^\beta h(1 - \phi). \tag{27}$$

The derivative of f_{el} at constant ϵ_B^α writes as

$$\begin{aligned}
 \left(\frac{\partial f_{el}}{\partial \phi} \right)_{\epsilon_B^\alpha} &= \left(f_{el}^\alpha - f_{el}^\beta \right) \frac{\partial h(\phi)}{\partial \phi} + \frac{\partial f_{el}^\alpha}{\partial \epsilon_n^\alpha} \frac{\partial \epsilon_n^\alpha}{\partial \phi} h(\phi) \\
 &\quad + \frac{\partial f_{el}^\beta}{\partial \epsilon_n^\beta} \frac{\partial \epsilon_n^\beta}{\partial \phi} h(1 - \phi). \tag{28}
 \end{aligned}$$

In order to determine, the derivatives of the non homogeneous variable with respect to the variation in the phase-field order

parameter ϕ , we utilize the expressions in Eq. (27). Since we require the partial derivatives at constant ϵ_B^α , it implies the differentiation of both sides in expression (27). It gives us the following relation

$$-(\epsilon_n^\alpha - \epsilon_n^\beta) \frac{\partial h(\phi)}{\partial \phi} = \frac{\partial \epsilon_n^\alpha}{\partial \phi} h(\phi) + \frac{\partial \epsilon_n^\beta}{\partial \phi} h(1 - \phi). \tag{29}$$

Rewriting Eq. (28), substituting the relation (29) and using the condition that, the normal components of stresses are homogeneous $\sigma_n = \partial f_{el}^\alpha / \partial \epsilon_n^\alpha = \partial f_{el}^\beta / \partial \epsilon_n^\beta$, the variational derivative simplifies as

$$\begin{aligned}
 \left(\frac{\partial f_{el}}{\partial \phi} \right)_{\epsilon_B^\alpha} &= \left(f_{el}^\alpha - f_{el}^\beta \right) \frac{\partial h(\phi)}{\partial \phi} \\
 &\quad + \left\langle \sigma_n, -(\epsilon_n^\alpha - \epsilon_n^\beta) \frac{\partial h(\phi)}{\partial \phi} \right\rangle. \tag{30}
 \end{aligned}$$

Reordering the particular components in Eq. (30), the derivative results as

$$\begin{aligned}
 \left(\frac{\partial f_{el}}{\partial \phi} \right)_{\epsilon_B^\alpha} &= \left[\left(f_{el}^\alpha - \langle \sigma_n, \epsilon_n^\alpha \rangle \right) - \left(f_{el}^\beta - \langle \sigma_n, \epsilon_n^\beta \rangle \right) \right] \frac{\partial h(\phi)}{\partial \phi} \\
 &= \left[\underbrace{\left(f_{el}^\alpha - \left\langle \frac{\partial f_{el}^\alpha}{\partial \epsilon_n^\alpha}, \epsilon_n^\alpha \right\rangle \right)}_{p^\alpha(\sigma_n, \epsilon_t)} \right. \\
 &\quad \left. - \underbrace{\left(f_{el}^\beta - \left\langle \frac{\partial f_{el}^\beta}{\partial \epsilon_n^\beta}, \epsilon_n^\beta \right\rangle \right)}_{p^\beta(\sigma_n, \epsilon_t)} \right] \frac{\partial h(\phi)}{\partial \phi} \\
 &= \frac{\partial}{\partial \phi} \left[p^\alpha(\sigma_n, \epsilon_t) h(\phi) + p^\beta(\sigma_n, \epsilon_t) h(1 - \phi) \right]. \tag{31}
 \end{aligned}$$

$p^\alpha(\sigma_n, \epsilon_t)$ and $p^\beta(\sigma_n, \epsilon_t)$ are bulk potentials, which include only homogeneous variables σ_n and ϵ_t . Both bulk potentials weighted with the smooth function $h(\phi)$ and $h(1 - \phi)$ correspondingly produce

$$P(\phi, \nabla\phi, \sigma_n, \epsilon_t) = p^\alpha(\sigma_n, \epsilon_t) h(\phi) + p^\beta(\sigma_n, \epsilon_t) h(1 - \phi). \tag{32}$$

The particular bulk potentials are composed of a Legendre transform of the bulk elastic energy density f_{el}^α with respect to ϵ_n^α

$$\begin{aligned}
 p^\alpha(\sigma_n, \epsilon_t) &= f_{el}^\alpha(\epsilon_n^\alpha(\sigma_n, \epsilon_t), \epsilon_t) \\
 &\quad - \left\langle \underbrace{\frac{\partial f_{el}^\alpha(\epsilon_n^\alpha(\sigma_n, \epsilon_t), \epsilon_t)}{\partial \epsilon_n^\alpha}}_{\sigma_n}, \epsilon_n^\alpha(\sigma_n, \epsilon_t) \right\rangle. \tag{33}
 \end{aligned}$$

and the corresponding part of β phase.

For the divergence part of the variation in Eq. (26), we calculate x -component of the derivative at a constant ϵ_B^α

$$\begin{aligned} \left(\frac{\partial f_{el}}{\partial \phi_x}\right)_{\epsilon_B^\alpha} &= f_{el}^\alpha \frac{\partial h(\phi)}{\partial \phi_x} + f_{el}^\beta \frac{\partial h(1-\phi)}{\partial \phi_x} \\ &+ \left(\frac{\partial f_{el}^\alpha}{\partial \epsilon_t} \frac{\partial \epsilon_t}{\partial \phi_x} h(\phi) + \frac{\partial f_{el}^\beta}{\partial \epsilon_t} \frac{\partial \epsilon_t}{\partial \phi_x} h(1-\phi)\right) \\ &+ \left(\frac{\partial f_{el}^\alpha}{\partial \epsilon_n^\alpha} \frac{\partial \epsilon_n^\alpha}{\partial \phi_x} h(\phi) + \frac{\partial f_{el}^\beta}{\partial \epsilon_n^\beta} \frac{\partial \epsilon_n^\beta}{\partial \phi_x} h(1-\phi)\right), \end{aligned} \tag{34}$$

with $\phi_x = (\nabla\phi)_x$. Similar expressions of the derivative results for the y and z components. Assuming isotropic bulk materials follow for material parameters $C_B^\alpha = C^\alpha$ and $C_B^\beta = C^\beta$. Since the material parameters are constant in the particular free energy density, the derivatives $\partial C^\alpha / \partial \phi_x = \partial C^\beta / \partial \phi_x = \mathbf{0}$ are zero. The first term of Eq. (34) is zero, because the interpolation function is independent of $\nabla\phi$. The partial derivatives are evaluated at constant $\epsilon_B^\alpha = (\epsilon_n, \epsilon_t)$, so that the derivative $\partial \epsilon_t / \partial \phi_x$ vanishes in Eq. (34). To evaluate the last term, we differentiate both sides of relation (27) with respect to ϕ_x at constant ϵ_n and have

$$0 = \left(\frac{\partial \epsilon_n^\alpha}{\partial \phi_x} h(\phi) + \frac{\partial \epsilon_n^\beta}{\partial \phi_x} h(1-\phi)\right). \tag{35}$$

Substituting the previous relation in Eq. (34) and using $\partial f_{el}^\alpha / \partial \epsilon_n^\alpha = \partial f_{el}^\beta / \partial \epsilon_n^\beta = \sigma_n$, we obtain $\partial f_{el} / \partial \nabla\phi = \mathbf{0}$. Therefore, the driving force part arising out of the divergence term $\nabla \cdot \partial f_{el} / \partial \phi_x$ is zero. Therefore the elastic contribution to the driving force equals to

$$\begin{aligned} \frac{\delta f_{el}}{\delta \phi} &= \frac{\partial P(\phi, \nabla\phi, \sigma_n, \epsilon_t)}{\partial \phi} \\ &= (p^\alpha(\sigma_n, \epsilon_t) - p^\beta(\sigma_n, \epsilon_t)) \frac{\partial h(\phi)}{\partial \phi}, \end{aligned} \tag{36}$$

with the potential $P(\phi, \nabla\phi, \sigma_n, \epsilon_t)$ as described in Eq. (32). For anisotropic bulk materials constants ($C_B^i \neq C^i$) an additional driving force contribution must be taken into account. Comparing the bulk densities p^i with the Eshelby Tensor for small deformations \mathbf{b} [15,21]

$$b_{kj} = f_{el}^\alpha \delta_{jk} - \sigma_{ij} \epsilon_{ik} \tag{37}$$

we notice, that the jump $[[p(\sigma_n, \epsilon_t)]]$ of the particular bulk densities $p^i(\sigma_n, \epsilon_t)$ is exactly equal to the jump of nn components of the Eshelby Tensor Eq. (37)

$$[[p(\sigma_n, \epsilon_t)]] \hat{=} \langle \mathbf{n}, [[\mathbf{b}]] \mathbf{n} \rangle. \tag{38}$$

2.5 Effective material parameters

The potential of the particular phase α defined only with continuous variables σ_n and ϵ_t is given by the Legendre transform of the elastic energy with respect to ϵ_n^α (see Eq. (33)). All the discontinuities are excluded from the variables and can be incorporated in the material parameter as presented in the following.

Using Eq. (24) results in the following derivative

$$\frac{\partial f_{el}^\alpha(\epsilon_n^\alpha, \epsilon_t)}{\partial \epsilon_n^\alpha} = C_{nn}^\alpha \epsilon_n^\alpha + C_{nt}^\alpha \epsilon_t = \sigma_n. \tag{39}$$

Reformulating the previous equation, we get an expression for the non-homogeneous variable

$$\epsilon_n^\alpha = (C_{nn}^\alpha)^{-1} (\sigma_n - C_{nt}^\alpha \epsilon_t). \tag{40}$$

The formulation of ϵ_n^α considers all shear components of the normal stresses σ_n and of the tangential strains ϵ_t . This makes the proposed approach more general in comparison with the proposed model by Durga et al. [3].

By inserting the expression (40) into (33), we get an energy term that is only dependent on homogeneous system variables

$$p^\alpha(\sigma_n, \epsilon_t) = \frac{1}{2} \left\langle (\sigma_n, \epsilon_t), \mathcal{T}^\alpha \begin{pmatrix} \sigma_n \\ \epsilon_t \end{pmatrix} \right\rangle, \tag{41}$$

with the material parameter matrix

$$\mathcal{T}^\alpha = \begin{pmatrix} -(C_{nn}^\alpha)^{-1} & (C_{nn}^\alpha)^{-1} C_{nt}^\alpha \\ (C_{nt}^\alpha)^T (C_{nn}^\alpha)^{-1} & C_{tt}^\alpha - (C_{nt}^\alpha)^T (C_{nn}^\alpha)^{-1} C_{nt}^\alpha \end{pmatrix}. \tag{42}$$

In order to get the total energy in the interface, we summarize the bulk energies $p^\alpha(\sigma_n, \epsilon_t)$ and $p^\beta(\sigma_n, \epsilon_t)$ that are weighted with the order parameter ϕ by multiplying with the smooth function $h(\phi)$ and $h(1-\phi) = 1-h(\phi)$, respectively. We define the homogeneous variable $\xi := (\sigma_n, \epsilon_t)^T$ and get

$$\begin{aligned} P(\phi, \nabla\phi, \xi) &= p^\alpha(\xi)h(\phi) + p^\beta(\xi)(1-h(\phi)) \\ &= \frac{1}{2} \left\langle \xi, \bar{\mathcal{T}} \xi \right\rangle. \end{aligned} \tag{43}$$

$\bar{\mathcal{T}}$ is thereby the linear interpolation of the material parameters

$$\bar{\mathcal{T}} = \mathcal{T}^\alpha(\nabla\phi)h(\phi) + \mathcal{T}^\beta(\nabla\phi)(1-h(\phi)). \tag{44}$$

The derivative of the potential $P(\phi, \nabla\phi, \xi)$ with respect to the homogeneous variable $\xi = (\sigma_n, \epsilon_t)^T$, yields the non homogeneous variable

$$\begin{aligned} \chi(\phi, \nabla\phi, \xi) &:= \frac{\partial P(\phi, \nabla\phi, \xi)}{\partial \xi} = \bar{\mathcal{T}}(\phi, \nabla\phi)\xi \\ &= \chi^\alpha h(\phi) + \chi^\beta (1 - h(\phi)). \end{aligned} \tag{45}$$

The sign of the normal component of χ changes due to the reverse Legendre transformation. $\bar{\mathcal{T}}$ is a new formulation of the proportionality tensor between the homogeneous variables $\xi = (\sigma_n, \epsilon_t)^T$ and their dependent counterparts $\chi = (-\epsilon_n, \sigma_t)^T$. The proportionality tensor is influenced by the interface orientation $\nabla\phi$ and the order parameter ϕ . Using the segmentation in Eq. (23) yields

$$\bar{\mathcal{T}} = \begin{pmatrix} \bar{\mathcal{T}}_{nn} & \bar{\mathcal{T}}_{nt} \\ \bar{\mathcal{T}}_{nt}^T & \bar{\mathcal{T}}_{tt} \end{pmatrix}, \tag{46}$$

where the parts are

$$\begin{aligned} \bar{\mathcal{T}}_{nn} &= -(C_{nn}^\alpha)^{-1}h(\phi) - (C_{nn}^\beta)^{-1}(1 - h(\phi)), \\ \bar{\mathcal{T}}_{nt} &= (C_{nn}^\alpha)^{-1}C_{nt}^\alpha h(\phi) + (C_{nn}^\beta)^{-1}C_{nt}^\beta(1 - h(\phi)), \\ \bar{\mathcal{T}}_{tt} &= \left(C_{tt}^\alpha - (C_{nt}^\alpha)^T (C_{nn}^\alpha)^{-1} C_{nt}^\alpha \right) h(\phi) \\ &\quad + \left(C_{tt}^\beta - (C_{nt}^\beta)^T (C_{nn}^\beta)^{-1} C_{nt}^\beta \right) (1 - h(\phi)). \end{aligned} \tag{47}$$

2.6 Incorporation of eigenstrains

The complexity of the proposed model increases, if we incorporate non-elastic strains $\tilde{\epsilon}^\alpha$ for the individual phase α into the system. The non-elastic strains can either be a constant eigenstrain ϵ_0^α , a plastic strain ϵ_{pl}^α , an eigenstrain dependent on the concentration $\epsilon_0^\alpha(c)$ or temperature $\epsilon_0^\alpha(T)$ or even the sum of different non-elastic strain contributions

$$\tilde{\epsilon}^\alpha = \epsilon_0^\alpha + \epsilon_{pl}^\alpha + \epsilon_0^\alpha(c) + \epsilon_0^\alpha(T) + \dots \tag{48}$$

Using the Voigt notation and the transformation in Eq. (10), the expression for the elastic energy Eq. (24) results in

$$f_{el}^\alpha(\epsilon_B^\alpha) = \frac{1}{2} \langle (\epsilon_B^\alpha - \tilde{\epsilon}_B^\alpha), C_B^\alpha (\epsilon_B^\alpha - \tilde{\epsilon}_B^\alpha) \rangle \tag{49}$$

Transforming the calculations in Sect. 2.5, we determine the components in n -direction by

$$\sigma_n = C_{nn}^\alpha (\epsilon_n^\alpha - \tilde{\epsilon}_n^\alpha) + C_{nt}^\alpha (\epsilon_t - \tilde{\epsilon}_t^\alpha), \tag{50}$$

$$\epsilon_n^\alpha = C_{nn}^{-1} (\sigma_n - C_{nt}^\alpha (\epsilon_t - \tilde{\epsilon}_t^\alpha)) + \tilde{\epsilon}_n^\alpha. \tag{51}$$

Replacing the whole dependence of ϵ_n^α in the elastic energy formulation (49) by the Legendre transformation results in a potential, which is only dependent on σ_n and ϵ_t

$$p^\alpha = \frac{1}{2} \left\langle (\sigma_n, \epsilon_t - \tilde{\epsilon}_t^\alpha), \mathcal{T}^\alpha \begin{pmatrix} \sigma_n \\ \epsilon_t - \tilde{\epsilon}_t^\alpha \end{pmatrix} \right\rangle - \langle \sigma_n, \tilde{\epsilon}_n^\alpha \rangle. \tag{52}$$

Separating the eigenstrain contribution in the previous expression reduces the potential to

$$\begin{aligned} p^\alpha(\sigma_n, \epsilon_t) &= \frac{1}{2} \left\langle (\sigma_n, \epsilon_t), \begin{pmatrix} \mathcal{T}_{nn}^\alpha & \mathcal{T}_{nt}^\alpha \\ \mathcal{T}_{nt}^{\alpha T} & \mathcal{T}_{tt}^\alpha \end{pmatrix} \begin{pmatrix} \sigma_n \\ \epsilon_t \end{pmatrix} \right\rangle \\ &\quad - \left\langle (\sigma_n, \epsilon_t), \begin{pmatrix} \mathbb{I} & \mathcal{T}_{nt}^\alpha \\ \mathbb{O} & \mathcal{T}_{tt}^\alpha \end{pmatrix} \begin{pmatrix} \tilde{\epsilon}_n^\alpha \\ \tilde{\epsilon}_t^\alpha \end{pmatrix} \right\rangle \\ &\quad + \frac{1}{2} \langle \tilde{\epsilon}_t^\alpha, \mathcal{T}_{tt}^\alpha \tilde{\epsilon}_t^\alpha \rangle. \end{aligned} \tag{53}$$

With $\xi = (\sigma_n, \epsilon_t)^T$, the corresponding result for the total elastic potential density is

$$P(\phi, \nabla\phi, \xi) = p^\alpha(\xi)h(\phi) + p^\beta(\xi)(1 - h(\phi)). \tag{54}$$

2.7 Calculation of stresses in diffuse interface systems

The formulation of the mixed energy is done in the base B given by the normal vector of the interface n and its tangential counterparts t and s . Now we derive the expression for stress depending on strain, which is given in the Cartesian coordinate system.

We start from the total elastic potential density in Eq. (54). The total strains in the normal direction ϵ_n are given by the derivative of the elastic potential density

$$\begin{aligned} \epsilon_n &= -\frac{\partial P(\phi, \nabla\phi, \xi)}{\partial \sigma_n} \\ &= -\bar{\mathcal{T}}_{nn}\sigma_n - \bar{\mathcal{T}}_{nt}\epsilon_t + \tilde{\chi}_n, \end{aligned} \tag{55}$$

with $\tilde{\chi}_n$ as the eigenstrain contribution in the normal direction

$$\tilde{\chi}_n := \left(\tilde{\epsilon}_n^\alpha + \mathcal{T}_{nt}^\alpha \tilde{\epsilon}_t^\alpha \right) h(\phi) + \left(\tilde{\epsilon}_n^\beta + \mathcal{T}_{nt}^\beta \tilde{\epsilon}_t^\beta \right) h(1 - \phi). \tag{56}$$

For the normal components of the stress σ_n , we obtain

$$\sigma_n = -\bar{\mathcal{T}}_{nn}^{-1} (\epsilon_n + \bar{\mathcal{T}}_{nt}\epsilon_t - \tilde{\chi}_n). \tag{57}$$

The tangential components of the stress tensor are given by the derivative

$$\sigma_t = \frac{\partial P(\phi, \nabla\phi, \xi)}{\partial \epsilon_t} = \bar{\mathcal{T}}_{nt}^T \sigma_n + \bar{\mathcal{T}}_{tt}\epsilon_t - \tilde{\chi}_t, \tag{58}$$

with $\tilde{\chi}_t$ as the eigenstress contribution in the tangential direction

$$\tilde{\chi}_t := \mathcal{T}_{tt}^\alpha \tilde{\epsilon}_t^\alpha h(\phi) + \mathcal{T}_{tt}^\beta \tilde{\epsilon}_t^\beta h(1 - \phi). \tag{59}$$

Replacing the normal component of σ by applying Eq. (57) results in the following equation for the tangential stresses

$$\sigma_t = -\bar{\mathcal{T}}_{nt}^T \bar{\mathcal{T}}_{nn}^{-1} (\epsilon_n + \bar{\mathcal{T}}_{nt}\epsilon_t - \tilde{\chi}_n) + \bar{\mathcal{T}}_{tt}\epsilon_t - \tilde{\chi}_t. \tag{60}$$

Using the Eqs. (57) and (60) leads to the stress components in expressed in base coordinate system

$$\begin{pmatrix} \sigma_n \\ \sigma_t \end{pmatrix} = \underbrace{\begin{pmatrix} -\bar{\mathcal{T}}_{nn}^{-1} & -\bar{\mathcal{T}}_{nn}^{-1}\bar{\mathcal{T}}_{nt} \\ -\bar{\mathcal{T}}_{nt}^T\bar{\mathcal{T}}_{nn}^{-1} & \bar{\mathcal{T}}_{tt} - \bar{\mathcal{T}}_{nt}^T\bar{\mathcal{T}}_{nn}^{-1}\bar{\mathcal{T}}_{nt}^T \end{pmatrix}}_{=: \mathcal{K}_B(\phi)} \begin{pmatrix} \epsilon_n \\ \epsilon_t \end{pmatrix} + \underbrace{\begin{pmatrix} \bar{\mathcal{T}}_{nn}^{-1} & \mathbb{O} \\ \bar{\mathcal{T}}_{nt}^T\bar{\mathcal{T}}_{nn}^{-1} & -\mathbb{I} \end{pmatrix}}_{=: \tilde{\sigma}_B} \begin{pmatrix} \tilde{\chi}_n \\ \tilde{\chi}_t \end{pmatrix}. \tag{61}$$

$\mathcal{K}_B(\phi)$ is the stiffness tensor and $\tilde{\sigma}_B(\phi)$ contains the eigenstresses in the transition region. Consequently the effective eigenstrains follow

$$\tilde{\epsilon}_B(\phi) = -[\mathcal{K}_B(\phi)]^{-1}\tilde{\sigma}_B(\phi). \tag{62}$$

Transforming this expression back to the Cartesian coordinate system using Eqs. (20) and (21), yields the effective stiffness and the effective eigenstrains in the transition region

$$\mathcal{K}(\phi) = M_\epsilon^T \mathcal{K}_B(\phi) M_\epsilon, \tag{63}$$

$$\tilde{\epsilon}^v(\phi) = M_\epsilon^T \tilde{\epsilon}_B(\phi). \tag{64}$$

We recover the Hook’s Law for the region of overlapping phases in the Voigt notation and Cartesian coordinate system

$$\sigma^v = \mathcal{K}(\phi) (\epsilon^v - \tilde{\epsilon}^v(\phi)), \tag{65}$$

with σ^v as the stress and ϵ^v the total strain in the Voigt notation, as defined in Eqs. (16) and (17).

3 Simulation results

In order to validate the proposed model, representative simulations are performed. The stress, strain and energy fields, which result from this, are compared to the analytical predictions and resulting fields using the Voigt/Taylor (VT) (1) and Reuss/Sachs (RS) (2) local homogenisation schemes. All simulations are performed using the release version 2.1 of the Pace3D package.

3.1 Serial and parallel material chains under tension

First we discuss a one-dimensional serial material chain shown on the left side in Fig. 1, with a diffuse transition region from the phase α to β in the center of the chain. Such a construction represents a two-phase sample with a sharp transition in the center. As boundary condition, we use constant stress in x-direction and zero stresses in other directions. Consequently, the stress in x-direction, which is the normal direction nn (see Eq. (9)) of the interface $\sigma_{xx} = \sigma_{nn} = \sigma_0$, is constant in mechanical equilibrium over the whole material chain. The resulting normal strain in the bulk is $\epsilon_{nn}^\alpha = \epsilon_{xx}^\alpha = \sigma_0/E_\alpha$ for the phase α and $\epsilon_{nn}^\beta = \epsilon_{xx}^\beta = \sigma_0/E_\beta$ for the phase β . With $E_\alpha = 0.1E_\beta$ as the corresponding Young’s modulus, the normal component of strain $\epsilon_{nn}^\alpha = 10\epsilon_{nn}^\beta$ follows with a jump at the position of

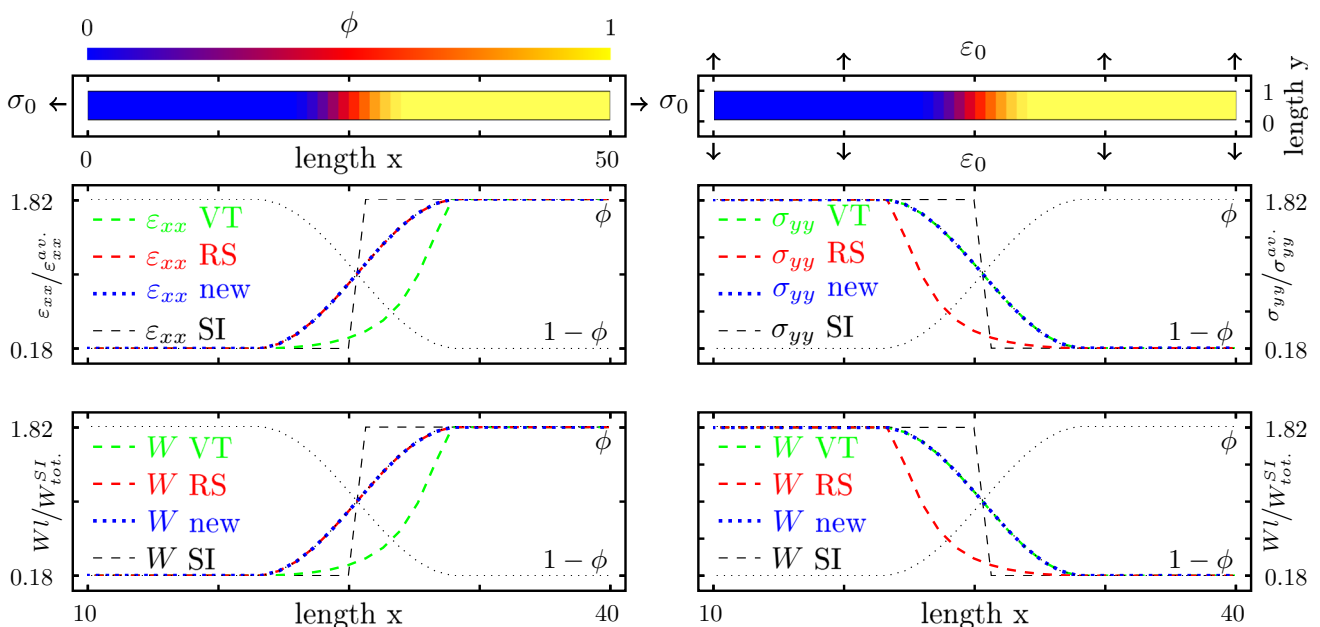


Fig. 1 Serial 1D material chain (left) and parallel 1D material chain (right). Constant stress σ_0 is applied in x-direction for the serial material chain and constant strain is applied in y-direction for the parallel chain. (Color figure online)

the sharp interface. In the case of a sharp interface, marked by superscript SI, the average normal strain of the sample $\epsilon_{nn}^{av.} = (\epsilon_{nn}^\alpha + \epsilon_{nn}^\beta)/2$ and the total mechanical energy result in $W_{tot.}^{SI} = l\epsilon_{nn}^{av.}\sigma_0/2 = 11l\sigma_0^2/(4E_\beta)$, with l as the length of the simulation domain. Consequently, a quantitative diffuse interface model should reproduce the strain and energy density jump in the center of the domain and the resulting total energy should be equal to $W_{tot.}^{SI}$. The left part of Fig. 1 shows the resulting strain ϵ_{nn} and mechanical energy density profiles W of the serial material chain derived with VT, RS and the proposed model. The strain and the energy density profiles of the RS and the proposed model follow exactly the corresponding volume fraction profile of the material, which is given by the order parameter ϕ . The position of strain and energy density jump is in the center of the simulation domain. The total energy, calculated by a line integral over the simulation domain, is $W_{tot.}^{RS} = W_{tot.}^{new} = W_{tot.}^{SI}$. The strain and energy density profile of VT does not match the ideal profile and the corresponding total energy deviates from the analytic value $W_{tot.}^{VT} \approx 0.9W_{tot.}^{SI}$.

On the right side of Fig. 1, the results of the parallel material chain are shown. The used boundary conditions are a constant strain ϵ_0 in y -direction, which is the tangential direction tt of the interface, and zero stress in other directions. The bulk tangential stresses are $\sigma_{tt}^\alpha = \sigma_{yy}^\alpha = E_\alpha\epsilon_0$ and $\sigma_{tt}^\beta = \sigma_{yy}^\beta = E_\beta\epsilon_0$ with a jump in the center of the material chain in the sharp interface description. The average tangential stress for the system is $\sigma_{tt}^{av.} = (\sigma_{tt}^\alpha + \sigma_{tt}^\beta)/2 = \epsilon_0(E_\alpha + E_\beta)/2$.

The total energy results in $W_{tot.}^{SI} = l\epsilon_0\sigma_{tt}^{av.}/2 = (11/4)l\epsilon_0^2$. The tangential stress and energy density profiles calculated with VT and the proposed method follow the corresponding volume fraction and the total energy is given by $W_{tot.}^{VT} = W_{tot.}^{new} = W_{tot.}^{SI}$. The profiles calculated with RS do not match the ideal line and consequently deviate the corresponding total energy from theoretical value $W_{tot.}^{RS} \approx 0.9W_{tot.}^{SI}$.

These one-dimensional simulations show that the assumption of constant strains in the diffuse interfacial region is only valid for the tangential components and that the assumption of constant stresses in the interface is only valid for the normal components.

3.2 Stress profiles of a plate with inclusion compared with theory

The simulations presented in Sect. 3.1 show that the proposed model describes the serial and parallel material chain exactly, where only the normal or tangential components of stresses and strains are acting, respectively. In order to validate the presented model in a more realistic system, we model a two-dimensional plate under plain strain conditions with a soft cylindrical inclusion under hydrostatic tension and compare the stress, strain and energy density fields, with theoretical predictions [22]. The simulation setup is shown in Fig. 2 top left. We insert a circular inclusion with a radius of $r = 100$ cells (1 cell = $1 \times 1\mu\text{m}$) in a simulation domain of 1300×1300 cells. The used width of the transition region

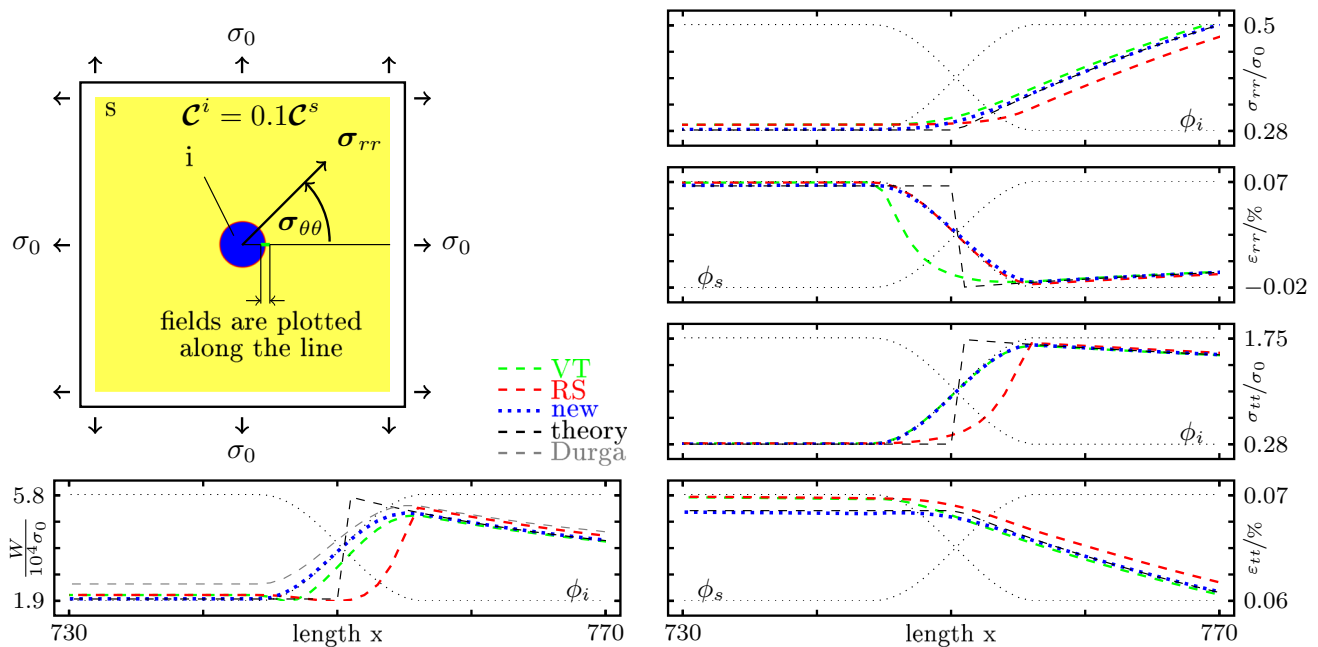


Fig. 2 Stress and strain profiles calculated with VT, RS and a proposed model of a plate with a soft cylindrical inclusion ($C^i = 0.1C^s$) under hydrostatic tension conditions compared with theoretical predictions [22]. The particular field profiles are plotted along the green line

pictured in the simulation setup on the top left side. For comparison the energy density profile calculated according to Durga et al. [3] (see Eq. (66)) is plotted. (Color figure online)

between the phases is $\lambda \approx 2.5\epsilon \approx 12$ cells. We choose an isotropic stiffness tensor with Young’s modulus $E_s = 210$ GPa for the plate, $E_i = 0.1E_s$ for the soft inclusion and an equal Poisson’s ratio for both phases $\nu_s = \nu_i = 0.3$. The hydrostatic tension is realized by a constant stress $\sigma_0 = 100$ MPa around the plate. In order to split the stress and strain fields in the normal and tangential components, we use the cylindrical coordinates for the underlying radial symmetric system. Thereby we can write $\sigma_{nn} = \sigma_{rr}$, $\epsilon_{nn} = \epsilon_{rr}$, $\sigma_{\theta\theta} = \sigma_{tt}$ and $\epsilon_{\theta\theta} = \epsilon_{tt}$. We evaluate the stress, strain and energy profiles in the transition zone between the solid and the inclusion. Therefore, we plot the corresponding field profiles, calculated with Voigt/Taylor, Reuss/Sachs, and the proposed model in comparison with theoretically predicted profiles along the green highlighted line in Fig. 2 top left.

We observe the same results as for the one-dimensional simulations in (Sect. 3.1). There is a deviation from the theoretically calculated profiles of the non homogenous variables σ_{tt} and ϵ_{rr} that are calculated using VT or RS methods respectively. The two-dimensional simulations show an additional deviation in the bulk phases for the homogenous variables σ_{nn} and ϵ_{tt} . These deviations in stresses and strains cause a deviation in the elastic potential energy W in the transition region, as well as in the bulk. The bulk energy deviation depends on the curvature κ and on the interface width λ . For the underlying simulation with $\kappa\lambda \approx 0.12$, we have a deviation of 7.3 % for VT and a deviation of 7.4 % for RV results. For a larger κ and λ product, e.g. $\kappa\lambda \approx 0.8$, the deviation is raised to 29 % for VT and 27 % for RS. The profiles of the homogenous and non homogenous variables, calculated with the proposed model, match very well with the theoretical predictions. Hence the deviation of bulk energy densities for $\kappa\lambda \approx 0.12$ is negligibly small (≈ 0.2 %). For $\kappa\lambda \approx 0.8$, which is an extreme value for a proper description of a curved interface, we get a deviation of ≈ 6 %.

As mentioned in the introduction, Durga et al. [3] presented a model where the stress and strain fields are calculated separately with VT and RS which then combine the corresponding strain and stress components for the energy calculation. Using this model, the energy density for the underlying radial symmetric system results in

$$W^{Durga} = \frac{1}{2} \left(\sigma_{rr}^{RS} \epsilon_{rr}^{s'} + \sigma_{tt}^{s'} \epsilon_{tt}^{VT} \right) h(\phi) + \frac{1}{2} \left(\sigma_{rr}^{RS} \epsilon_{rr}^{i'} + \sigma_{tt}^{i'} \epsilon_{tt}^{VT} \right) h(1 - \phi). \tag{66}$$

Thereby, the non homogeneous variables are defined as [3]

$$\sigma_{tt}^{s'} = \frac{C_{tttt}^s \epsilon_{tt}^{VT} + C_{rrtt}^s S_{rrrr}^s \sigma_{rr}^{RS}}{1 - C_{rrtt}^s S_{rrrr}^s}, \tag{67}$$

$$\epsilon_{rr}^{s'} = \frac{S_{rrrr}^s \sigma_{rr}^{RS} + S_{rrtt}^s C_{tttt}^s \epsilon_{tt}^{VT}}{1 - C_{rrtt}^s S_{rrrr}^s} \tag{68}$$

and the corresponding components for the inclusion. As shown in Fig. 2 energy density W^{Durga} provides the expected energy profile in the transition region. However, the profile does not match the theoretical value within the inclusion. This deviation is caused by the deviation of σ_{rr}^{RS} and ϵ_{tt}^{VT} , which serve as the basis for the calculation of W^{Durga} (see Eq. (66)).

3.3 Validation of the driving force

For solidification processes, Kim et al. [16], Plapp [17] Choudhury and Nestler [18] pointed out, that using a potential which only uses homogenous variables avoid the interfacial excess energy. Durga et al. [3] have shown, that also in the case of elasticity, there is an excess energy in the interface and they have demonstrated their impact [3]. In order to demonstrate that the proposed model does not produce an energy excess in the interface, we generate one-dimensional equilibrium states for the serial and parallel material chain. The simulation setups are the same as the ones we used in Sect. 3.1. In addition, we calculate the evolution of the order parameter given by Eq. (4) with the elastic contribution to the driving force given by Eq. (36).

For the case of serial material chains, the equilibrium conditions are $\sigma_{nn}^\alpha = \sigma_{nn}^\beta$ and $p^\alpha(\xi) = p^\beta(\xi)$. The first condition is fulfilled by the chosen boundary conditions $\sigma_{nn}^\alpha = \sigma_{nn}^\beta = \sigma_0$. Due to the underlying one-dimensional problem, the particular energy density given by Eq. (53) decreases to

$$p^\alpha(\xi) = \frac{1}{2} \left(\sigma_{nn} [-\mathbf{C}^\alpha]_{nnnn}^{-1} \sigma_{nn} \right) - \sigma_{nn} \tilde{\epsilon}_{nn}^\alpha = \frac{1}{2} \sigma_0 \left(-S_{nnnn}^\alpha \sigma_0 - 2\tilde{\epsilon}_{nn}^\alpha \right). \tag{69}$$

Assuming that the eigenstrain in the softer phase is zero $\tilde{\epsilon}_{nn}^\beta = 0$, the eigenstrain in the α phase for serial material chain follows from the second equilibrium condition reading

$$p^\alpha(\sigma_{nn}) = p^\beta(\sigma_{nn}) \\ \frac{1}{2} \sigma_0 \left(-S_{nnnn}^\alpha \sigma_0 - 2\tilde{\epsilon}_{nn}^\alpha \right) = -\frac{1}{2} \sigma_0 S_{nnnn}^\beta \sigma_0 \\ \implies \tilde{\epsilon}_{nn}^\alpha = \frac{1}{2} \left(S_{nnnn}^\beta - S_{nnnn}^\alpha \right) \sigma_0. \tag{70}$$

Figure 3 pictures the strain and ϕ equilibrium profiles in the left diagrams. The order parameter profile calculated with RS and proposed model follow the initial ϕ profile. The resulting interface width λ is equal to the theoretical value $\lambda = \pi^2 \epsilon / 4 \approx 2.5\epsilon$. The solution calculated with VT model shows a deviation in ϵ_{nn} and ϕ from the ideal profile.

In the case of parallel material chain, the equilibrium conditions change to $\epsilon_{tt}^\alpha = \epsilon_{tt}^\beta = \epsilon_0$ and $p^\alpha(\xi) = p^\beta(\xi)$. With

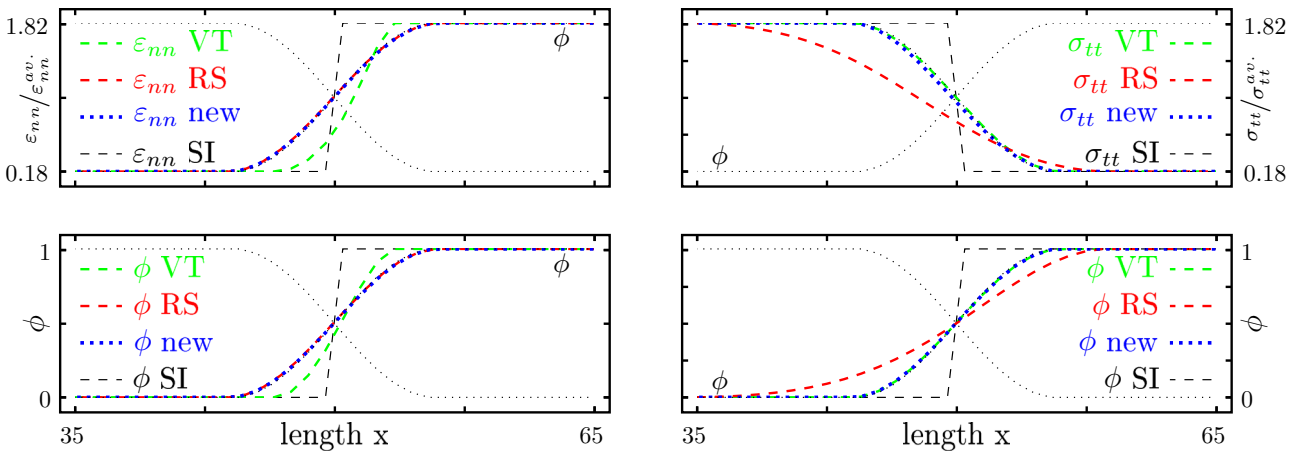


Fig. 3 Equilibrium profiles of ϕ and ϵ_{nn} correspondingly σ_{tt} for the serial (left) and parallel (right) material chain calculated with VT, RS and the proposed new model. The chosen nondimensionalized initial

surface energy $\gamma_0 = 5 \times 10^{-3}$ for the serial and $\gamma_0 = 4 \times 10^{-6}$ for the parallel material chain. (Color figure online)

the assumption $\tilde{\epsilon}_{nn}^\beta = 0$ and the equality of bulk energy densities, the following set of equations hold

$$\begin{aligned}
 p^\alpha(\epsilon_{tt}) &= p^\beta(\epsilon_{tt}) \\
 \frac{1}{2}\epsilon_0^2 C_{tttt}^\alpha - C_{tttt}^\alpha \epsilon_0 \tilde{\epsilon}_{tt} + \frac{1}{2} C_{tttt}^\alpha \tilde{\epsilon}_{tt}^2 &= \frac{1}{2}\epsilon_0^2 C_{tttt}^\beta \\
 \implies \tilde{\epsilon}_{tt}^\alpha &= \epsilon_0 \left(1 - \sqrt{\frac{C_{tttt}^\beta}{C_{tttt}^\alpha}} \right). \tag{71}
 \end{aligned}$$

The resulting σ_{tt} and ϕ equilibrium profiles are pictured in Fig. 3 on the right. While the equilibrium ϕ profiles calculated with VT and the proposed model are equal to the initial ϕ profile, the equilibrium ϕ profile calculated with RS model becomes broader.

The reason for the change of equilibrium interface widths λ_{eq} is the elastic interfacial excess energy. Kim et al. [16] and Cha et al. [23] pointed out the role of interfacial excess energy and calculated the equilibrium interface width λ and surface energy γ for solidification in binary systems. For the presented model we obtain

$$\lambda = \int_0^1 \frac{d\phi}{\sqrt{\frac{16}{\pi^2}\phi(1-\phi) + \frac{\epsilon}{\gamma_0} \Delta P(\phi, \nabla\phi, \xi)}}, \tag{72}$$

$$\gamma = 2\gamma_0 \int_0^1 \sqrt{\frac{16}{\pi^2}\phi(1-\phi) + \frac{\epsilon}{\gamma_0} \Delta P(\phi, \nabla\phi, \xi)} d\phi, \tag{73}$$

with $\Delta P(\phi, \nabla\phi, \xi) = P(\phi, \nabla\phi, \xi) - p^\alpha(\xi) - p^\beta(\xi)$ as the elastic energy density difference between values at the interface and that of the bulk phases. Durga et al. [3] calculated and illustrated the elastic contribution to interfacial excess energy for different interface widths. For the proposed model the elastic contribution of interfacial energy excess of a one-dimensional two phase domain is defined as

$$\begin{aligned}
 W_{el}^{xs} &= \int_{-\infty}^{\infty} P(\phi, \nabla\phi, \xi) - p^\alpha(\xi) - p^\beta(\xi) dx \\
 &= \int_{-\infty}^{\infty} \Delta P(\phi, \nabla\phi, \xi) dx. \tag{74}
 \end{aligned}$$

Applying Eqs. (72), (73) and (74) to other models, the energy density $P(\phi, \nabla\phi, \xi)$ has to be replaced correspondingly. For an odd profile $P(\phi, \nabla\phi, \xi)$, which is antisymmetric at $\phi = 0.5$, the elastic interfacial energy excess W_{el}^{xs} vanishes and we retrieve the expected values for $\lambda = \pi^2 \epsilon / 4$ and $\gamma = \gamma_0$. Each deviation from this profile leads to an excess energy contribution $W_{el}^{xs} \neq 0$, which distorts the equilibrium ϕ and which in turn modifies the resulting interface width λ and surface energy γ , according to Eqs. (72), (73). Figure 4 images this context. An elastic energy density profile which is antisymmetric at the $\phi = 0.5$ point changes the equilibrium interface width and surface energy. The energy profile of the serial chain calculated with VT model or the energy profile of parallel chain calculated with RS model (see Fig. 1), are elastic energy densities with non antisymmetric profiles at the $\phi = 0.5$ isoline. We find a change of both, the interface width as well as the surface energy. Using an energy density, which depends only on homogenous variables, avoids an energy excess in the interface and the expected values for λ and γ follow. This context is shown and applied to solidification processes by Choudhury and Nestler [18]. The proposed model uses the homogenous variable $\xi = (\sigma_n, \epsilon_t)^T$ in the formulation of $P(\phi, \nabla\phi, \xi)$, see Eq. (43). All discontinuities are incorporated in the material parameter $\mathcal{T}(\phi, \nabla\phi)$. The excess energy W_{el}^{xs} vanishes and the equilibrium ϕ profile does not distort in a stationary solution of Eq. (4), as pictured in Fig. 3 for parallel and serial material chain. Consequently, the elastic contribution to the driving force does not modify the equilibrium values of λ and γ , as shown in Fig. 3 for a mount of W^α/γ_0 ratios.

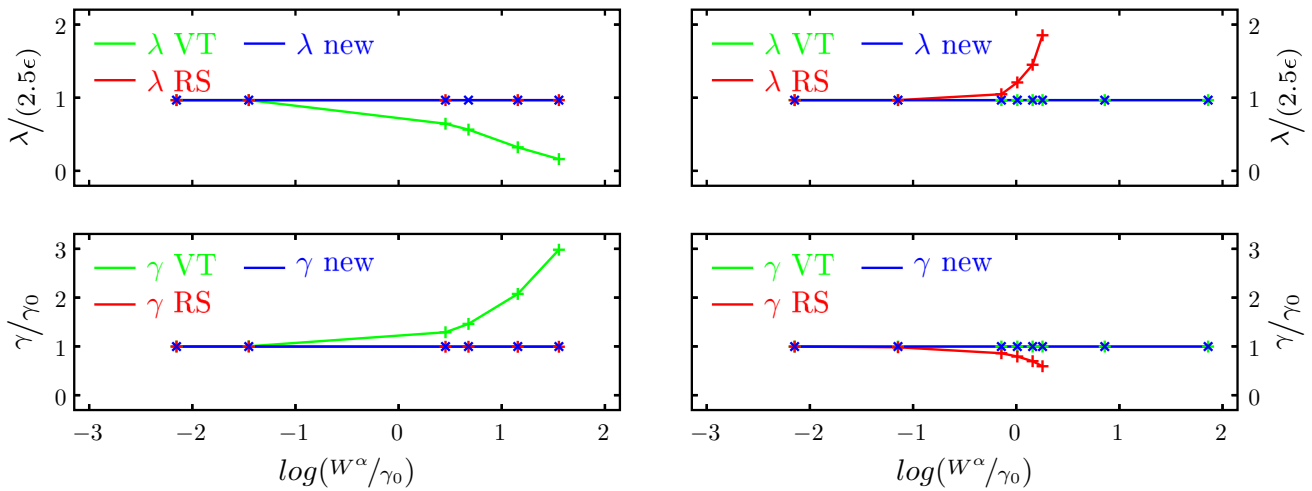


Fig. 4 Equilibrium interface widths λ and corresponding surface energies γ for the serial (left) and parallel (right) material chains with varying initial surface energy γ_0 . (Color figure online)

3.4 2D equilibrium through Gibbs–Thomson effect

In two dimensions, an interfacial equilibrium condition can be reached using the Gibbs–Thomson effect. For a circular inclusion of radius r_i , embedded in a matrix material, an equilibrium is reached, if the surface energy is equal to the potential energy. Such a condition satisfies the following local condition [4,24,25]

$$\omega^s - \omega^i - \left\langle \left(\epsilon_n^s - \epsilon_n^i \right), \sigma_n^i \right\rangle = 2\bar{\kappa} \Gamma_{si}, \tag{75}$$

where ω^s, ω^i are the grand canonical energy densities of the solid and the inclusion respectively. $\bar{\kappa} = 1/r_i$ is the mean curvature and Γ_{si} is the excess grand canonical energy density at the transition surface. $\epsilon_n^s - \epsilon_n^i = \llbracket \epsilon_n \rrbracket$ is the jump of strains and σ_n the corresponding stress component in the normal direction of the transition surface. The present investigation concentrates on the mechanical contribution, thus the jump of grand canonical energy densities reduces to the jump of elastic energy density $\omega^s - \omega^i = \llbracket \omega \rrbracket = \llbracket W_{el} \rrbracket$ at the sharp interface transition surface. For purely elastic systems, the Gibbs–Thomson Eq. (75) reduces to

$$\llbracket W_{el} \rrbracket - \left\langle \llbracket \epsilon_n \rrbracket, \sigma_n^i \right\rangle = \frac{1}{r_i} \gamma_{si}^{eq}, \tag{76}$$

with γ_{si} as the surface energy density. The left part of the previous expression is nothing else then the difference of particular Eshelby Tensors (see Eq. (37)) in nn direction. As already mentioned in Sect. 2.4 jump of the Eshelby Tensors in nn direction $\langle n, \llbracket b \rrbracket n \rangle$ is equal to the jump of bulk densities $\llbracket p(\sigma_n, \epsilon_t) \rrbracket$. It comes as no surprise, that in a sharp interface limit, the elastic contribution of the Gibbs–Thomson Eq. (76)

is exactly equal to the elastic driving force contribution of the proposed model $\partial P(\phi, \nabla \phi, \sigma_n, \epsilon_t) / \partial \phi$.

We choose the simulation setup of Sect. 3.2. Furthermore we use the theoretically predicted stress fields of Mai and Singh [22] and calculate the equilibrium surface energy density γ_{si}^{eq} according to Eq. (76)

$$\gamma_{si}^{eq}(r_i) = \frac{r_i}{2} \left(\llbracket \sigma_{\theta\theta}^{th}(r_i) \rrbracket \epsilon_{\theta\theta}^{th}(r_i) - \sigma_{rr}^{th}(r_i) \llbracket \epsilon_{rr}^{th}(r_i) \rrbracket \right). \tag{77}$$

$\epsilon_{\theta\theta}^{th}(r_i)$ and $\sigma_{\theta\theta}^{th}(r_i)$ are the theoretical values at the transition surface. The theoretical description of Mai and Singh [22] for the underlying problem requires a load σ_∞ , which acts in infinity. In order to fit this value we compare the outer energy of the simulation with the energy of theoretical description at appropriate distance. Thereby we have ensured, that the outer energies of the simulation and the theoretical description are equal. This condition is satisfied for $\sigma_\infty = 1.009712\sigma_0$ and a chosen value of $\sigma_0 = 100$ MPa in the simulation.

Figure 5 (left) shows the energy field near the equilibrium condition calculated with the proposed model. The growth or shrinkage plot of the inclusion for different surface energy densities γ_{si} is shown on the right. This plot demonstrates the quantity of the proposed driving force including 2D structures and curved surfaces. The elastic driving force of our model is consistent with the theoretically predicted ones, described by Eq. (77).

4 Conclusion

In this paper, we present a quantitative elasticity phase-field model for solid–solid systems. Despite the diffuse interface, which is indispensable for the phase-field models, the method satisfies the mechanical jump conditions. Comparing the

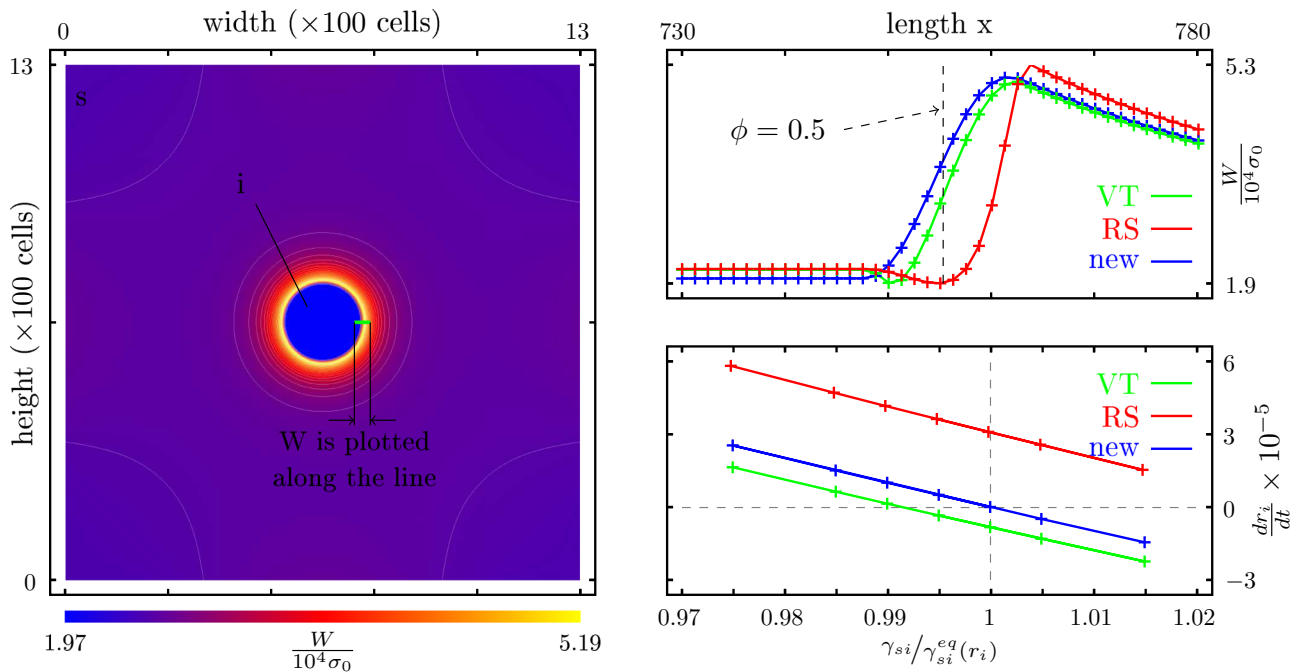


Fig. 5 2D validation of the proposed model over the Gibbs–Thomson effect. The computed energy field is shown on the *left*. The energy profiles on *top right* refer to simulations, which satisfy the condition

simulated stress profiles in a plate with a round inclusion under hydrostatic tension with theoretically predicted stress fields, we show the quantitative characteristics of the resulted fields. The presented one dimensional equilibrium simulations demonstrate the quantity of the elastic driving force contribution and show the limits of VT and RS model. Both the interface width as well as the surface energy remain stable at equilibrium applying the proposed model regardless of the elastic driving force contribution. The two-dimensional equilibrium simulations, according to the Gibbs–Thomson effect, demonstrate the quantity of the proposed elastic driving force contribution on curved surfaces. We show a connection of the formulated bulk potentials with the Eshelby Tensor and demonstrate, that the proposed elastic driving force contribution is exactly equal to the elastic contribution of the Gibbs–Thomson equation.

Additionally we offer the possibility to calculate the stresses for the particular phase $\sigma_B^\alpha = (\sigma_n, \sigma_t^\alpha)^T$ in the transition region. The normal component is equal for both phases and the tangential component is given by

$$\sigma_t^\alpha = \frac{\partial p^\alpha(\sigma_n, \epsilon_t)}{\partial \epsilon_t}, \tag{78}$$

with $p^\alpha(\sigma_n, \epsilon_t)$ as described in Eq. (53). The quantitative stresses of the particular phase is important to solve the yield criterion in order to calculate plastic strain. For example the Prandtl–Reuss model [26] with von Mises yield criterion and linear isotropic hardening approximation can be used. The

$\gamma_{si}/\gamma_{si}^{eq}(r_i) = 1$ and which are plotted along the *green marked line*. The growth or shrinkage of the inclusion for different surface energy densities γ_{si} are shown in the *bottom right diagram*. (Color figure online)

coupling of the resulted phase dependent plastic strain ϵ_{pl}^α with the proposed model is straightforward using Eq. (48).

Acknowledgments We thank the DFG for funding our investigations in the framework of the Research Training Group 1483. The work was further supported by the state Baden-Wuerttemberg and European Fonds for regional development with a center of excellence in Computational Materials Science and Engineering and by Helmholtz Portfolio topic “Materials Science for Energy and its Applications in Thin Film Photovoltaics and in Energy Efficiency”.

Appendix

Transformation of stresses and strains in Voigt notation

In the Voigt notation, the strains and stresses can be written as

$$\sigma^v = (\sigma_{11}, \sigma_{22}, \sigma_{33}, \sigma_{23}, \sigma_{13}, \sigma_{12})^T, \tag{79}$$

$$\epsilon^v = (\epsilon_{11}, \epsilon_{22}, \epsilon_{33}, 2\epsilon_{23}, 2\epsilon_{13}, 2\epsilon_{12})^T. \tag{80}$$

Then, the transformation (10) becomes $\sigma_B^v = M_\sigma^v \sigma^v$, with the transformation matrix

$$M_\sigma^v = \begin{pmatrix} n_1n_1 & n_2n_2 & n_3n_3 & 2n_2n_3 & 2n_1n_3 & 2n_1n_2 \\ t_1t_1 & t_2t_2 & t_3t_3 & 2t_2t_3 & 2t_1t_3 & 2t_1t_2 \\ s_1s_1 & s_2s_2 & s_3s_3 & 2s_2s_3 & 2s_1s_3 & 2s_1s_2 \\ t_1s_1 & t_2s_2 & t_3s_3 & t_2s_3+t_3s_2 & t_1s_3+t_3s_1 & t_1s_2+t_2s_1 \\ n_1s_1 & n_2s_2 & n_3s_3 & n_2s_3+n_3s_2 & n_1s_3+n_3s_1 & n_1s_2+n_2s_1 \\ n_1t_1 & n_2t_2 & n_3t_3 & n_2t_3+n_3t_2 & n_1t_3+n_3t_1 & n_1t_2+n_2t_1 \end{pmatrix}. \tag{81}$$

An analogue transformation for the strain can be written as $\epsilon_B^v = M_\epsilon^v \epsilon^v$, with the transformation matrix

$$M_\epsilon^v = \begin{pmatrix} n_1n_1 & n_2n_2 & n_3n_3 & n_2n_3 & n_1n_3 & n_1n_2 \\ t_1t_1 & t_2t_2 & t_3t_3 & t_2t_3 & t_1t_3 & t_1t_2 \\ s_1s_1 & s_2s_2 & s_3s_3 & s_2s_3 & s_1s_3 & s_1s_2 \\ 2t_1s_1 & 2t_2s_2 & 2t_3s_3 & t_2s_3+t_3s_2 & t_1s_3+t_3s_1 & t_1s_2+t_2s_1 \\ 2n_1s_1 & 2n_2s_2 & 2n_3s_3 & n_2s_3+n_3s_2 & n_1s_3+n_3s_1 & n_1s_2+n_2s_1 \\ 2n_1t_1 & 2n_2t_2 & 2n_3t_3 & n_2t_3+n_3t_2 & n_1t_3+n_3t_1 & n_1t_2+n_2t_1 \end{pmatrix}. \tag{82}$$

We reorder the components of the strain and stress vectors and define

$$\epsilon_B^\alpha := \left(\underbrace{\epsilon_{nn}, \epsilon_{ns}, \epsilon_{nt}}_{\epsilon_n}, \underbrace{\epsilon_{tt}, \epsilon_{ss}, \epsilon_{ts}}_{\epsilon_t} \right)^T = (\epsilon_n, \epsilon_t)^T, \tag{83}$$

$$\sigma_B^\alpha := \left(\underbrace{\sigma_{nn}, \sigma_{ns}, \sigma_{nt}}_{\sigma_n}, \underbrace{\sigma_{tt}, \sigma_{ss}, \sigma_{ts}}_{\sigma_t} \right)^T = (\sigma_n, \sigma_t)^T. \tag{84}$$

Due to this reformulation, we permute the rows of the previous matrices M_σ^v and M_ϵ^v , but the named properties remain

$$M_\sigma = \begin{pmatrix} n_1n_1 & n_2n_2 & n_3n_3 & 2n_2n_3 & 2n_1n_3 & 2n_1n_2 \\ n_1t_1 & n_2t_2 & n_3t_3 & n_2t_3+n_3t_2 & n_1t_3+n_3t_1 & n_1t_2+n_2t_1 \\ n_1s_1 & n_2s_2 & n_3s_3 & n_2s_3+n_3s_2 & n_1s_3+n_3s_1 & n_1s_2+n_2s_1 \\ t_1t_1 & t_2t_2 & t_3t_3 & 2t_2t_3 & 2t_1t_3 & 2t_1t_2 \\ s_1s_1 & s_2s_2 & s_3s_3 & 2s_2s_3 & 2s_1s_3 & 2s_1s_2 \\ t_1s_1 & t_2s_2 & t_3s_3 & t_2s_3+t_3s_2 & t_1s_3+t_3s_1 & t_1s_2+t_2s_1 \end{pmatrix}, \tag{85}$$

$$M_\epsilon = \begin{pmatrix} n_1n_1 & n_2n_2 & n_3n_3 & n_2n_3 & n_1n_3 & n_1n_2 \\ 2n_1t_1 & 2n_2t_2 & 2n_3t_3 & n_2t_3+n_3t_2 & n_1t_3+n_3t_1 & n_1t_2+n_2t_1 \\ 2n_1s_1 & 2n_2s_2 & 2n_3s_3 & n_2s_3+n_3s_2 & n_1s_3+n_3s_1 & n_1s_2+n_2s_1 \\ t_1t_1 & t_2t_2 & t_3t_3 & t_2t_3 & t_1t_3 & t_1t_2 \\ s_1s_1 & s_2s_2 & s_3s_3 & s_2s_3 & s_1s_3 & s_1s_2 \\ 2t_1s_1 & 2t_2s_2 & 2t_3s_3 & t_2s_3+t_3s_2 & t_1s_3+t_3s_1 & t_1s_2+t_2s_1 \end{pmatrix}. \tag{86}$$

This follows the transformations of stresses and strains as used in Eqs. (20) and (21).

5 Driving force contributions of VT and RS model

The main assumption of the VT scheme [1] is that the strains of overlapping phases are equal. In a two phase system with ϕ_α and ϕ_β , the corresponding volume fractions follow Eq. (1) for the stress σ^{VT} . The energy density results accordingly to [9–11]

$$\begin{aligned} f_{el}^{VT}(\phi, \epsilon) &= f_{el}^\alpha(\epsilon)h(\phi) + f_{el}^\beta(\epsilon)(1-h(\phi)) \\ &= \frac{1}{2} \left((\epsilon - \tilde{\epsilon}^\alpha, \mathbf{C}^\alpha(\epsilon - \tilde{\epsilon}^\alpha))h(\phi) \right. \\ &\quad \left. + (\epsilon - \tilde{\epsilon}^\beta, \mathbf{C}^\beta(\epsilon - \tilde{\epsilon}^\beta))(1-h(\phi)) \right). \end{aligned} \tag{87}$$

Using Eq. (4), the corresponding contribution of the driving force for the VT model is given by

$$\begin{aligned} \Delta f_{el}^{VT}(\phi, \epsilon) &= \frac{1}{2} \left((\epsilon - \tilde{\epsilon}^\beta, \mathbf{C}^\beta(\epsilon - \tilde{\epsilon}^\beta)) \right. \\ &\quad \left. - (\epsilon - \tilde{\epsilon}^\alpha, \mathbf{C}^\alpha(\epsilon - \tilde{\epsilon}^\alpha)) \right) \frac{\partial h(\phi)}{\partial \phi}. \end{aligned} \tag{88}$$

The assumption of the RS model is that the stresses are equal for the two overlapping phases. The system variables are now changed from strains to stresses. The corresponding elastic potential of phase α for such a system can be derived by changing the system variable in Eq. (87) with the Legendre transformation to the form

$$f_{el}^{RS}(\phi, \sigma) = f_{el}^{VT}(\phi, \epsilon) - \frac{\partial f_{el}^{VT}(\phi, \epsilon)}{\partial \epsilon} \epsilon. \tag{89}$$

This results in

$$\begin{aligned} f_{el}^{RS} &= \frac{1}{2} \left(\sigma^{RS}, (\mathbf{S}^\beta(1-h(\phi)) - \mathbf{S}^\alpha h(\phi)) \sigma^{RS} \right) \\ &\quad - \left(\sigma^{RS}, \tilde{\epsilon}^\alpha h(\phi) + \tilde{\epsilon}^\beta(1-h(\phi)) \right), \end{aligned} \tag{90}$$

with σ^{RS} given in Eq. (2). The corresponding contribution of the driving force for the RS model can be expressed as

$$\begin{aligned} \Delta f_{el}^{RS}(\phi, \sigma) &= \left(\frac{1}{2} \left(\sigma^{RS}, (\mathbf{S}^\alpha - \mathbf{S}^\beta) \sigma^{RS} \right) \right. \\ &\quad \left. + \left(\sigma^{RS}, \tilde{\epsilon}^\alpha - \tilde{\epsilon}^\beta \right) \right) \frac{\partial h(\phi)}{\partial \phi}. \end{aligned} \tag{91}$$

References

- Voigt W (1889) Über die Beziehung zwischen den beiden Elastizitätskonstanten isotroper Körper. Annalen der Physik 274(12):573
- Reuss A (1929) Berechnung der Fließgrenze von Mischkristallen auf Grund der Plastizitätsbedingung für Einkristalle. Z Angew Math Mech 9:49
- Durga A, Wollants P, Moelans N (2013) Evaluation of interfacial excess contributions in different phase-field models for elastically inhomogeneous systems. Model Simul Mater Sci Eng 21(5):055018
- Johnson WC, Alexander JID (1986) Interfacial conditions for thermomechanical equilibrium in two-phase crystals. J Appl Phys 59(8):2735
- Moelans N, Blanpain B, Wollants P (2008) An introduction to phase-field modeling of microstructure evolution. Calphad 32(2):268
- Chen LQ (2002) Phase-field models for microstructure evolution. Annu Rev Mater Res 32(1):113
- Ammar K, Appolaire B, Cailletaud G, Forest S (2009) Combining phase field approach and homogenization methods for modelling phase transformation in elastoplastic media. Revue européenne de mécanique numérique 18(5–6):485
- Khachaturyan A (1983) Theory of structural transformation in solids. Wiley, New York

9. Spatschek R, Müller-Gugenberger C, Brener E, Nestler B (2007) Phase field modeling of fracture and stress-induced phase transitions. *Phys Rev E* 75(6):1
10. Mennerich C, Wendler F, Jainta M, Nestler B (2011) A phase-field model for the magnetic shape memory effect. *Arch Mech* 63:549
11. Schneider D, Schmid S, Selzer M, Böhlke T, Nestler B (2014) Small strain elasto-plastic multiphase-field model. *Comput Mech* 55(1):27–35
12. Schneider D, Selzer M, Bette J, Rementeria I, Vondrous A, Hoffmann MJ, Nestler B (2014) Phase-field modeling of diffusion coupled crack propagation processes. *Adv Eng Mater* 16(2):142–146
13. Steinbach I, Apel M (2006) Multi phase field model for solid state transformation with elastic strain. *Physica D* 217:153
14. Apel M, Benke S, Steinbach I (2009) Virtual dilatometer curves and effective young's modulus of a 3D multiphase structure calculated by the phase-field method. *Comput Mater Sci* 45(3):589
15. Silhavy M (1997) *The mechanics and thermodynamics of continuous media*, 1997th edn. Springer, Berlin
16. Kim SG, Kim WT, Suzuki T (1999) Phase-field model for binary alloys. *Phys Rev E* 60(6 Pt B):7186
17. Plapp M (2011) Unified derivation of phase-field models for alloy solidification from a grand-potential functional. *Phys Rev E* 84(3):031601
18. Choudhury A, Nestler B (2012) Grand Potential formulation for multi-component phase transformations combined with thin-interface asymptotics of the double obstacle potential. *Phys Rev E Stat Nonlinear Soft Matter Phys*, pp 1–36
19. Nestler B, Garcke H, Stinner B (2005) Multicomponent alloy solidification: phase-field modeling and simulations. *Phys Rev E* 71(4):1
20. Slawinski MA (2010) *Waves and rays in elastic continua*, 2nd edn. World Scientific Pub Co, London
21. Gross D, Seelig T (2011) *Bruchmechanik: Mit einer Einführung in die Mikromechanik*. Springer, Berlin
22. Mai AK, Singh SJ (1991) *Deformation of elastic solids*. Prentice Hall, Englewood Cliffs
23. Cha PR, Yeon DH, Yoon JK (2001) A phase field model for isothermal solidification of multicomponent alloys. *Acta Mater* 49(16):3295–3307
24. Voorhees PW, Johnson WC (1986) Interfacial equilibrium during a first-order phase transformation in solids. *J Chem Phys* 84(9):5108
25. Johnson WC (1987) Precipitate shape evolution under applied stress thermodynamics and kinetics. *Metall Trans A* 18(2):233–247
26. Simo J, Hughes T (1998) *Computational inelasticity*. Springer, New York